Jerzy Nowacki, Adam Sajek

Numerical Simulation of the Thermal Cycle of the PAW-MAG Hybrid Welding of Advanced High Strength Steels

Abstract: The research described in the article was concerned with the possibility of determining time $t_{8/5}$ using the Finite Element Method. The research-related tests involved a joint made of AHSS S960QL using the PAW-MAG method. Values of time $t_{8/5}$ were compared in relation to characteristic zones of the joint and constant heat input values. Differences in cooling rates related to the diversified geometry of a joint and the asymmetric distribution of heat proved significant. The research involved the identification of possibilities offered by the Finite Element Method involving space modelling in the examination of the thermal history of any welded joint area. The comparison of the analysed manner of determining time $t_{8/5}$ with traditional measurement and analytical methods revealed the significant advantage of the FEM consisting in the accurate and complete induction of a cycle in the entire cross-section of the joint in contrast with experimental contact and non-contact methods averaging the measurement on the joint surface or only in the weld axis. In view of differences related to time $t_{8/5}$ reaching 1.5 seconds in the joint area and the very narrow range of the tolerance concerning the value of the cooling time of AHSS, the Finite Element Method involving the use of space modelling was recognised as a necessary tool when designing welded joints made of Advanced High Strength Steels.

Keywords: numerical analysis of welding, welding thermal cycle, hybrid welding, quenched and tempered Ahss, HPAW, FEM, simulation, cooling rate

Introduction

The use of advanced materials in numerous structures favours the dynamic development of welding techniques [1, 2]. Presently used welding processes are characterised by a significant number of variables affecting the final result. More important welding process characteristics include a heat input and a welding thermal cycle, affecting the structural transformations, properties as well as the stresses and strains of welded structures. The determination of temperature changes at a predefined point of a joint using conventional measurements is a complex process supported by FEM-based computer-aided software applications dedicated to welding. On the basis of the adequate definition of all process components, the above-named software programmes make it possible to identify

prof. dr hab. inż. Jerzy Nowacki (Professor PhD (DSc) Hab. Eng.), dr inż. Adam Sajek (PhD (DSc) Eng.) – West Pomeranian University of Technology in Szczecin, Department of Welding

temperature distribution as well as determine stresses and strains in welded joints. A welding technology designed in the above-presented manner only requires being subjected to a limited experiment verifying the correctness of calculations [3, 4].

Time $t_{8/5}$ in the Analysis of Welding Thermal Cycles of AHSS

An important attribute conditioning the properties of welded joints is the time of cooling within the temperature range of 800°C to 500°C ($t_{8/5}$). Depending on the dynamics of cooling, the temperature range of 800°C to 500°C is the range where varied structural transformations affecting joint properties take place. For each steel grade, some minimum and maximum values of $t_{8/5}$ are allowed (Fig. 1). The range of recommended AHSS-related times $t_{8/5}$ becomes visibly narrowed, primarily by reducing the maximum value, which results from the transformations of the microstructure formed in steelmaking processes [5, 6].

In cases of Advanced High Strength Steels (AHSS), not only time $t_{8/5}$, but also the time of cooling from 500°C to 200°C is of particular importance due to the fact that the martensitic transformation and martensite hardening

Fig. 1. Recommended times $t_{8/5}$ for fine-grained structural steels [6]

occur in the lower range of the above-presented temperature range. For this reason, in the case under discussion the analysis of the welding thermal cycle should include the entire range of cooling temperature [7 ÷ 13]. Time $t_{8/5}$ is affected by thermal parameters of materials, joint geometry (particularly joint thickness), initial temperature and a heat input to the joint. A heat input can be identified experimentally based on measurements of temperature distribution in the joint during post-weld cooling, yet such an identification is a complex issue as the methods used for measurements of temperature distribution in joints (contact methods involving the use of thermocouples or contactless methods, e.g. pyrometric or thermovision) are encumbered with errors related to measurement methods [14 ÷ 16]. Time $t_{8/5}$ can also be determined analytically based on formulas taking into account welding parameters. The multitude of mathematical dependences enabling the identification of cooling rates significantly limits the versatility of the method.

Heat Distribution in PAW-MAG Hybrid Welding

The research involved tests aimed to demonstrate the efficiency of the Finite Element Method in measurements of time $t_{8/5}$. The tests involved the use of the simufact.welding software programme being a specialised computational FEM environment dedicated to welding applications. The programme performs calculations for dynamically changing process heat parameters in transient conditions and, in doing so, takes into consideration complete temperature-dependent material characteristics and phase transformations occurring at preset cooling rates. In addition, the programme enables the definition of types and sizes of heat sources which can be concentrated in cases of laser and plasma welding processes or more dissipated, e.g. double-ellipsoidal in cases of SMAW, GTAW and GMAW welding processes. The performance of calculations required the creation
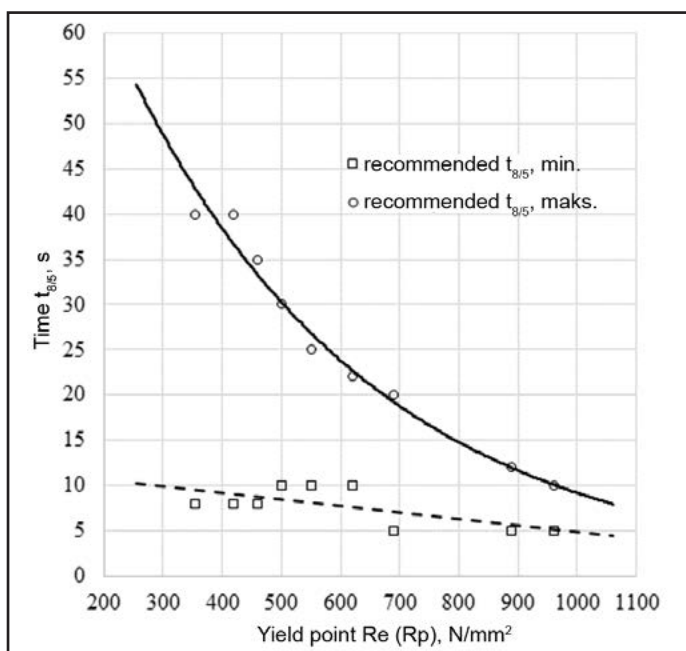
of the 3D model of the joints using other programmes, i.e.:

– Solidworks 2015 (CAD environment) – as regards the creation of 2D geometry based on the macroscopic photograph of a model welded joint;
– midas NFX 2015 (FEM multi-task environment) – as regards the creation of three spatial finite element meshes on the basis of flat geometry (two meshes for the sheets and one mesh for the weld).

The research-related tests involved the performance of the simulation of heat distribution during PAW-MAG hybrid welding combining the processes of plasma arc welding (PAW) with GMAW. The PAW-MAG welding method is characterised by high welding rates and the possibility of the single-layer welding of thick joints. The parameters adopted for individual heat sources were the following: plasma polarity: DC-; plasma arc voltage: 28.0 V; plasma current: 340 A; plasma gas flow rate: 4.0 l/min; MAG polarity: DC+; MAG arc voltage: 33.0 V; MAG current: 345 A and filler metal wire (ϕ 1.0 mm) feeding rate: 10 m/min. For a welding rate of 75 cm/min and the efficiency of both arcs being 80%, a heat input to the joint amounted to 13.4 kJ/cm. The simulation was performed for a welded joint of a variable sheet thickness, characteristic of crane jib structures, where the lower, i.e., rounded part of the shape transmitting greater loads had a thickness of 7.0 mm, and the upper part, providing appropriate rigidity, had a thickness of 5.0 mm. The joint was subjected to V-bevelling without a gap. The length of the joint amounted to 120.0 mm, whereas the width of the sheets amounted to 50.0 mm. Pre-heating was not applied.

The research involved the identification of a hybrid heat source composed of plasma arc reproduced by the model of a concentrated source and MAG arc reproduced by the model of a conventional source (double ellipsoid). For the concentrated source, the adopted diameter of the primary cylinder of concentrated heat amounted to 4.0 mm, whereas the height amounted to 7.5 mm (joint thickness). The diameter of heat effect cylinder amounted to 6.0 mm, whereas the depth of effect amounted to 3.0 mm. The adopted heat distribution amounted to 50/50 for both cylinders.

The area width adopted for the conventional source amounted to 4.0 mm, the front part of the model amounted to 2.0 mm, whereas the rear part amounted to 6.0 mm. The identified depth of the temperature field amounted to 5.0 mm. It was decided that, due to the inclination of the MAG welding head in the direction of plasma arc, the distribution of heat would be greater in the front part of the model. Both heat sources were moved by 2.0 mm from the joint axis in the direction of the thinner sheet and inclined by an angle of 12° so that arc would be concentrated on the thicker sheet. The distance between the heat sources amounted to 8.0 mm. The material used in the tests corresponded (in terms of chemical composition and properties) to steel s960QL (belonging to AHSS).
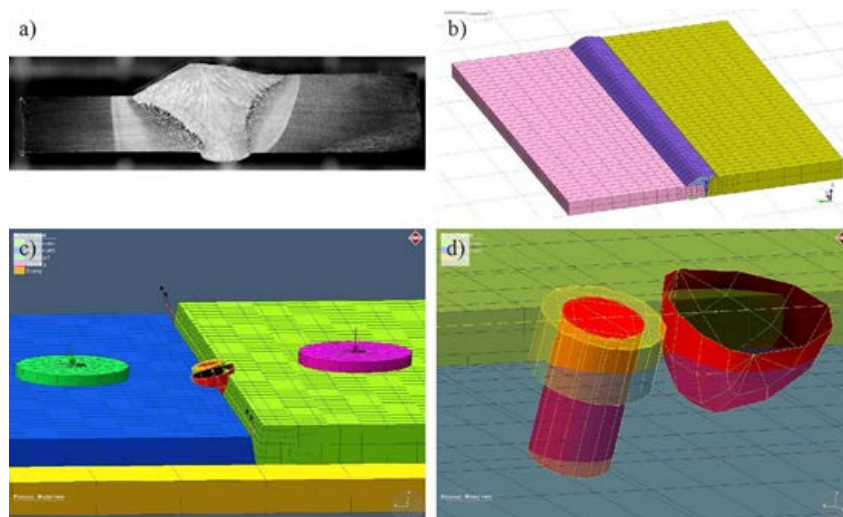
Fig. 2. Geometry of the joint and method of the modelling the hybrid heat source: a) macroscopic image of the welded joint of 5.0 mm and 7.0 mm thick sheets b) space model of the joint – the finite element mesh in the midas NFX software programme; c) definition of the welding process in the simufact.welding software programme allowing for support, the pressure of each of the welded plates and the appropriate trajectory for the heat source; d) geometry of the hybrid heat source
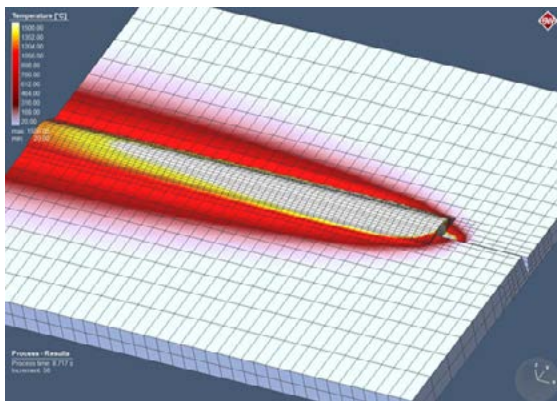
Fig. 3. Simulation of the hybrid welding of stainless steel S960QL joint using the simufact.welding software programme and the condensation of the finite element mesh within the heat source
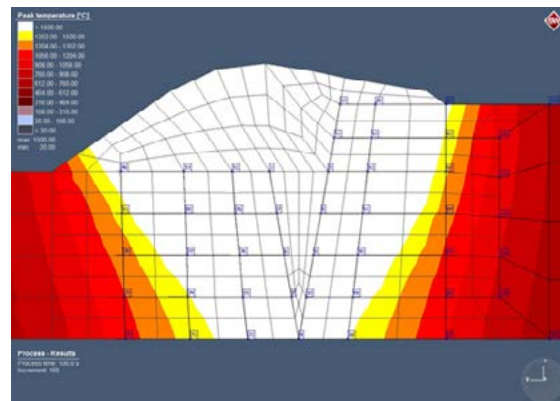
Fig. 4. Distribution of maximum temperatures in the welded joint and the measurement points for which the temperature values were recorded in the function of time

The simulation involved a period of 100 seconds including the time of welding process and of cooling, where the time of welding amounted to 10.3 s. The increase in the accuracy of calculations required the double condensation of the finite element mesh around the heat source (Fig. 3). The analysis involved the cross-section of the joint at the half of its length; selected measurement points were located at two depths in the weld and HAZ (Fig. 4). The above named points were used to plot the curves of temperature in the function of time, which, in turn, were used to determine the vales of $t_{8/5}$ in the individual areas of the joint (Table 1).

The simulation enabled the identification of cooling times within the temperature range of 800°C to 500°C in relation to the analysed points of the welded joint. The cooling times were restricted within the range of 8.1 s to 9.6 s. The lowest value of $t_{8/5}$ was observed in the weld axis in the thinner sheet. This fact can be attributed to the inclination of the welding head aimed at the more effective heating of the thicker sheet. The longest time $t_{8/5}$ was identified in relation to the area distant from the fusion

Table 1. Numbers of selected nodes and measurement points (in the parentheses) lying on the cross-section of the welded joint subjected to analysis (L - weld face area; G – weld root area; LW - fusion line area; LW + 2 mm - area approx. 2 mm away from the fusion line)

| Sheet thickness, mm | Area subjected to analysis | | | | | |
| | Weld - axis | | Weld - LW | | HAZ | |
	L	G	L	G	LW	LW + 2 mm
7,0	3 (9)	10 (21)	82 (7)	89 (22)	83 (11)	86 (23)
5,0	1 (29)	5 (41)	49 (32)	74 (43)	81 (36)	75 (44)

Table 2. Values of time $t_{8/5}$ in the measurement points; L –weld face area; G – weld root area; LW – fusion line area; LW + 2 mm - area approx. 2 mm away from the fusion line

| Sheet thickness, mm | Area subjected to analysis | | | | | |
| | Weld - axis | | Weld - LW | | HAZ | |
	L	G	L	G	LW	LW + 2 mm
7.0	8.3	8.5	9.4	8.9	9.4	9.6
5.0	8.1	8.6	8.7	8.6	8.8	9.0
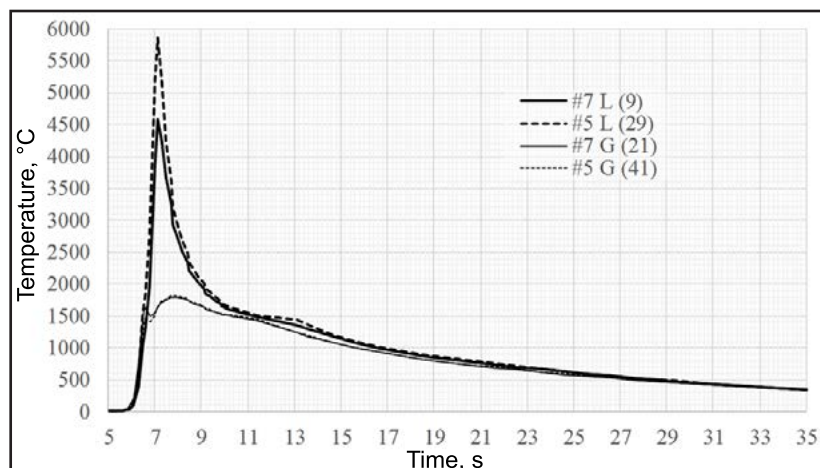
Fig. 5. Temperature changes in the weld axis #7/#5 - sheet thickness, mm; L – weld face area, G – weld root area

line in the thicker sheet. The high value of $t_{8/5}$ resulted from the greater amount of heat concentrated in the thicker material and the lower cooling rate of the area distant from the weld. Because of the high gradient of temperature and intense bidirectional heat discharge to elements being joined, the joint area characterised by the fastest cooling was the weld centre. The increase in the distance from the weld axis was accompanied by the decrease in the cooling rate and the extension of $t_{8/5}$, which significantly affected the character of structural transformations in these areas.

The methodology enabling the simulation of welding processes using space modelling was applied when implementing the process of PAW-MAG hybrid welding in industry. It was possible to observe a high coincidence of simulation results with technological data obtained when making a model joint in laboratory conditions as well as high accuracy and resolution of time $t_{8/5}$ measurement in relation to the cross-section of the welded joint (to be discussed in the subsequent article).

Fig. 6. Temperature changes in the weld at the fusion line; #7/#5 - sheet thickness; mm; L – weld face area, G – weld root area
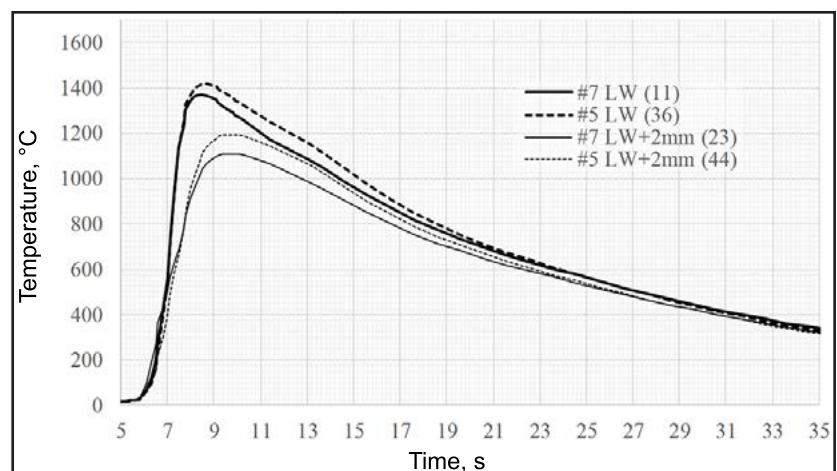
Fig. 7. Temperature changes in the HAZ; #7/#5 - sheet thickness; mm; L – weld face area, LW – fusion line area

Summary

– The numerical simulation of the thermal cycle of PAW–MAG hybrid welding (characterised by the unique geometry of the weld pool) of Advanced High Strength Steels (AHSS) using space modelling is an effective tool in the analysis of the thermal history of any area of a complex-structured joint and can constitute the basis for the analysis of heat distribution, microstructure, properties, stresses and strains as well as can enable the assessment of welding technology parameters and, at the structure design stage, make it possible to identify the favourable variants of welded joints.

– The advantage of the simulation of welding processes involving space modelling over contact-based and contactless temperature measurement method averaging measurements on the joint surface or only in the weld axis consists in the precise and complex induction of a thermal cycle on the entire cross-section of a joint.

– Time $t_{8/5}$ amounted to 8.1 s ÷ 9.6 s; the time of further cooling within the temperature range of 500°C to 200°C was considerably longer, which significantly affected the character of transformations in the joint made of AHSS at temperatures below 500°C.

– The simulation of heat distribution during the PAW-MAG hybrid welding of AHSS, including the entire range of thermal cycle temperature from the welding temperature to the ambient

temperature, constitutes a tool for the analysis of diffusive and diffusionless transformations at temperatures below 500°C.

– In view of time $t_{8/5}$-related differences amounting to 1.5 s in the joint area and the narrow range of tolerances related to cooling times of AHSS, the FEM involving space modelling should be recognised as an indispensable tool when designing joints made of Advanced High Strength Steels.

References

[1] Shome M., Tumuluru M.: *Welding and Joining of Advanced High Strength Steels (AHSS)*, 1st Edition, 2015, pp. 93-119
http://dx.doi.org/10.1016/b978-0-85709-436-0.00001-1

[2] Porter D. A.: *Weldable High-Strength Steels: Challenges and Engineering Applications*. IIW International Conference High-Strength Materials - Challenges and Applications, 2-3 July 2015, Helsinki, Finland

[3] Hwang S. Y., Kim Y., Lee J. H.: *Finite element analysis of residual stress distribution in a thick plate joined using two-pole tandem electro-gas welding*. Journal of Materials Processing Technology, 2016, vol. 229, pp. 349-360
http://dx.doi.org/10.1016/j.jmatprotec.2015.09.037

[4] Májlinger K., Kalácska E., Spena P.R.: *Gas Metal Arc Welding of Dissimilar AHSS Sheets*. Materials & Design, 2016, vol. 109, pp. 615-621
http://dx.doi.org/10.1016/j.matdes.2016.07.084

[5] Banerjee K.: Improving weldability of an advanced high strength steel by design of base metal microstructure. Journal of Materials Processing Technology, 2016, vol. 229, pp. 596-608
http://dx.doi.org/10.1016/j.jmatprotec.2015.09.026

[6] Tijden A.: *(Delta $t_{8/5}$) S355 t/m S960*
http://www.certilas.nl/nl/content/afkoel-tijden-delta-t85-s355-tm-s960

[7] Liu W., Ma W., Yang G., Kovacevic R.: *Hybrid laser-arc welding of advanced high-strength steel*. Journal of Materials Processing Technology, 2014, 214, pp. 2823-2833
http://dx.doi.org/10.1016/j.jmatprotec.2014.06.018

[8] Nowacki J., Krajewski S., Matkowski P.: *PTA-GMA hybrid welding of UHSS steel in structures of large-scale*. Arch. of Materials Science and Eng., 2015, vol. 71, no. 2, pp. 53-62

[9] Nowacki J., Krajewski S.: *Dual-phase steels microstructure and properties consideration based on artificial intelligence techniques*. Archives of Civil and Mechanical Engineering, 2014, vol. 14, no. 2, pp. 278–286
http://dx.doi.org/10.1016/j.acme.2013.10.002

[10] Krajewski S., Nowacki J.: *Modelowanie właściwości dwufazowych stali DP z zastosowaniem sztucznej inteligencji*. Inżynieria Materiałowa, 2012, no. 6, pp. 372-376

[11] Krajewski S., Nowacki J.: *Dual-phase steels microstructure and properties consideration based on artificial intelligence techniques*. Archives of Civil and Mechanical Engineering, 2014, vol. 14, no. 2, pp. 278-286
http://dx.doi.org/10.1016/j.acme.2013.10.002

[12] Nowacki J., Sajek A., Matkowski P.: *Welding of MART steel with the use of matching fillers*. Archives of Materials Science, 2014, vol. 70, no. 2, pp. 77–86

[13] Nowacki J., Sajek A., Matkowski P.: *The influence of welding heat input on the microstructure of joints of S1100QL steel in one-pass welding*. Archives of Civil and Mechanical Engineering, 2016, no. 16, pp. 777-783
http://dx.doi.org/10.1016/j.acme.2016.05.001

[14] Reisgen M., Schleser O., Mokrov E.: *Statistical modeling of laser welding of DP/TRIP steel sheets*. Optics & Laser Technology, 2012, vol. 44, pp. 92-101
http://dx.doi.org/10.1016/j.optlastec.2011.05.025

[15] Long N. P., Matsunaga Y., Hanari T., Yamada T., Muramatsu T.: *Experimental investigation of transient temperature characteristic in high power fiber laser cutting of a thick steel plate*. Optics & Laser Technology, 2016, vol. 84, pp. 134-143
http://dx.doi.org/10.1016/j.optlastec.2016.05.005

[16] Kube C. M.: *Attenuation of laser generated ultrasound in steel at high temperatures; comparison of theory and experimental measurements*. 70 Ultrasonics, 2016, pp. 238-240
http://dx.doi.org/10.1016/j.ultras.2016.05.009